

## Research Article

# Mullite Reinforced SiC/Al<sub>2</sub>O<sub>3</sub> Composites Prepared by Microwave Sintering Based on Green Manufacturing

Xudan Dang <sup>1</sup>, Shaojie Shi,<sup>2</sup> Linjun Li,<sup>3</sup> Fei Luo,<sup>1</sup> and Zheng Ding<sup>1</sup>

<sup>1</sup>School of Mechanical Engineering, Henan University of Engineering, Zhengzhou 451191, China

<sup>2</sup>Finance and Asset Management Division, Henan University of Engineering, Zhengzhou 451191, China

<sup>3</sup>Engineering Training Centre, Henan University of Engineering, Zhengzhou 451191, China

Correspondence should be addressed to Xudan Dang; dangxudan2011@163.com

Received 15 May 2022; Accepted 27 June 2022; Published 9 July 2022

Academic Editor: Conghu Liu

Copyright © 2022 Xudan Dang et al. This is an open access article distributed under the Creative Commons Attribution License, which permits unrestricted use, distribution, and reproduction in any medium, provided the original work is properly cited.

In the preparation process of composites, the implementation of green manufacturing technology has an important impact on improving material properties and preparation efficiency. The adopting of green manufacturing technology not only greatly reduces the energy consumption but also effectively avoids the environmental pollution. Compared with the traditional material preparation process, the material preparation process for green manufacturing is a new concept and idea. Microwave sintering is such an efficient, clean, and pollution-free preparation process, so it is widely used in the field of material preparation. By microwave sintering, the mullite reinforced SiC/Al<sub>2</sub>O<sub>3</sub> composites with different SiC particle size were prepared from the composite powders composed of SiC particles coated with SiO<sub>2</sub>, by a sol-gel method and Al<sub>2</sub>O<sub>3</sub> particles. The effect of SiC particle size on the microstructure, bulk density, fracture toughness, flexural strength, and thermal shock resistance of SiC/Al<sub>2</sub>O<sub>3</sub> composites was studied. The bulk density, fracture toughness, and flexural strength were evaluated by the Archimedes method, single-side notched beam method, and three-point bending method, respectively. The thermal shock resistance of samples was investigated through the combination of water quenching and three-point bending methods. The results showed that with the increase of SiC particle size, the bulk density, fracture toughness, and flexural strength of samples all increased first and then decreased. The bulk density, fracture toughness, flexural strength, and flexural strength retention of SiC(5 μm)/Al<sub>2</sub>O<sub>3</sub> composites were better than those of other samples, which were 2.06 g/cm<sup>3</sup>, 1.98 MPa·m<sup>1/2</sup>, 63 MPa, and 60%, respectively. The better mechanical properties and thermal shock resistance of SiC(5 μm)/Al<sub>2</sub>O<sub>3</sub> composites are due to the formation of bridging mullite whiskers between SiC and Al<sub>2</sub>O<sub>3</sub> particles with large length diameter ratio. Therefore, the unique sintering mechanisms of size coupling effect and local thermal aggregation effect in microwave sintering were discussed. The research results can not only provide reference for the preparation process of mullite reinforced SiC/Al<sub>2</sub>O<sub>3</sub> composites but also for the wide application of microwave sintering technology.

## 1. Introduction

With the rapid development of science and technology, the manufacturing industry has also received more development opportunities, which not only creates greater economic value for the society, but also brings more economic benefits to the development of the society [1]. However, with the rapid development of traditional manufacturing industry, problems such as high energy consumption and high pollution gradually appear. The environment-friendly manufacturing process based on green manufacturing has

become the development direction in the future. The green manufacturing of composites is an important innovation and development in the research field of composite preparation technology. Green manufacturing is also known as environmental conscious manufacturing for environment [2, 3]. Low energy consumption green preparation process is also called energy-saving process in general [4]. Compared with traditional material preparation, material preparation based on green manufacturing is a new concept and idea [5]. Microwave sintering is a new method of material sintering process. It has the characteristics of fast heating speed, high

energy utilization rate, high heating efficiency, safety, sanitation, and no pollution. Because the time of microwave sintering is greatly shortened, the energy utilization efficiency is greatly improved. Compared with traditional sintering methods, microwave sintering can achieve high efficiency and energy saving. The rapid sintering characteristics of microwave sintering greatly reduce the use of gas as sintering atmosphere in the sintering process, which not only reduces the cost but also reduces the emission of waste gas and waste heat in the sintering process. As one of the green manufacturing processes, microwave sintering is worthy of its name. At the same time, microwave sintering can improve the microstructure and properties of sintered materials, which has become a new research hotspot in the field of material sintering.

Microwave sintering is a method to realize densification, by coupling the special band of microwave with the basic fine structure of materials to generate heat, and the dielectric loss of materials makes the whole material heated to the sintering temperature. In the 1960s, some researchers proposed to use microwave sintering technology to prepare ceramic materials. After the mid-1980s, there was a climax of microwave sintering ceramics all over the world [6]. So far, researchers have done a lot of research on the preparation of carbide ceramics and oxide ceramics by microwave sintering technology [7, 8]. Because of the excellent high temperature mechanical strength, superior refractoriness, low electrical conductivity, good chemical stability, and good thermal shock resistance, the SiC/Al<sub>2</sub>O<sub>3</sub> composites have become a promising candidate for high-temperature applications in the fields of refractory materials, machinery, chemical industry, metallurgy, electronics, and ceramics [9, 10]. However, in the fields of several thermal shocks or applications requiring high toughness, the SiC/Al<sub>2</sub>O<sub>3</sub> composites are unsuitable for their brittleness [11, 12]. In order to make the SiC/Al<sub>2</sub>O<sub>3</sub> composites tougher, some reinforcing phase is introduced into the composites to overcome their inherent brittleness. Not only the morphology of the reinforcing phase but also the chemical compatibility and thermal expansion match of the reinforcing phase and matrix could influence the preparation process and final properties of SiC/Al<sub>2</sub>O<sub>3</sub> composites. The recent research showed that particles and whiskers can greatly improve the strength and toughness of the ceramic matrix composites [13–16]. For whisker reinforced composites, the improvement is due to the changes of the microstructure, interface strengthening, and fracture mechanisms. Mullite whiskers are widely used to enhance the properties of alumina-based composites. The in situ mullite whiskers can be synthesized by coating SiO<sub>2</sub> on SiC particles, which facilitates the reaction between SiO<sub>2</sub> and Al<sub>2</sub>O<sub>3</sub> to form mullite whiskers at high temperature. The connections of mullite whiskers improve the interfacial bonding between SiC and Al<sub>2</sub>O<sub>3</sub> particles. In addition, the oxidation problem of SiC particles in the sintering process is also solved through the coating of SiO<sub>2</sub> in SiC particles. For SiC/Al<sub>2</sub>O<sub>3</sub> composites, many reports indicated that mullite whiskers show attractive bending strength at high temperature, good thermal shock resistance, and excellent chemical compatibility with SiC [17–19]. Thus, due to their excellent

thermal shock resistance, mullite whisker reinforced SiC/Al<sub>2</sub>O<sub>3</sub> composites have broad application prospects, especially in refractories.

Using various processing techniques such as pressureless sintering, hot pressing, and microwave sintering, the mullite reinforced SiC/Al<sub>2</sub>O<sub>3</sub> composites can be prepared. As an internal and faster technique, microwave sintering has received more attention compared with traditional sintering methods [20–22]. Besides being a green manufacturing process, microwave sintering also has two advantages. One is the volumetric energy absorption without temperature gradient over the entire sample. And the other is some special properties induced by the electromagnetic field [23]. Furthermore, besides the improvement of quality of the composites, the microwave sintering can also bring time and energy savings for its unique heating behavior [24, 25]. In addition to increasing the heating rate, uniform heating, and energy saving, microwave sintering also makes the composites have higher density and mechanical properties [26, 27]. Bodhak studied the sintering of pure mullite and mullite-zirconia composites and the results show that compared with the conventional sintering, the microwave sintering leads to better densification and better mechanical [28].

Nevertheless, so far, there were few reports about the preparation of in situ mullite whisker reinforced SiC/Al<sub>2</sub>O<sub>3</sub> composites, especially on the microstructure, properties, and microwave sintering mechanism of the composites. In the present investigation, the SiC/Al<sub>2</sub>O<sub>3</sub> composites reinforced by in situ mullite were prepared. In the previous research, the optimum sintering temperature, holding time, volume fraction of SiC particles, and volume fraction of Al<sub>2</sub>O<sub>3</sub> particles about the mullite reinforced SiC/Al<sub>2</sub>O<sub>3</sub> composites were 1500°C, 30 min, 50%, and 50%, respectively [14]. Therefore, the above sintering parameters were also used here. The effect of SiC particle size on the microstructure and properties of mullite reinforced SiC/Al<sub>2</sub>O<sub>3</sub> composites were studied in details. Furthermore, the mechanism of microwave sintered SiC/Al<sub>2</sub>O<sub>3</sub> composites were discussed, compared with the conventional sintering.

## 2. Experimental Method

*2.1. Microwave Sintering Equipment.* Microwave sintering furnace is the key equipment of microwave sintering. The microwave sintering furnace used in this study was shown in Figure 1. Its model is WXD20S-07 (Nanjing Sanle Microwave equipment) multimode microwave sintering furnace, with a maximum input power of 10 kw, frequency of 2.45 GHz, and resonant cavity mode of TE<sub>666</sub>. The microwave furnace is mainly composed of microwave emission source, microwave conduction system, multimode resonator, microwave detection, feedback system, and infrared temperature measurement system.

In order to quickly complete the sintering and reduce the heat loss of samples in microwave sintering, a thermal insulation structure based on a hybrid heating mode was used to isolate the samples from the external environment [29]. The thermal insulation structure, which was mainly



(a)



(b)

FIGURE 1: The resonant cavity and control panel of microwave sintering equipment uniformity of samples. And at the same time the disadvantages that the temperature of samples close to the SiC rods in the insulation structure was high, and the temperature away from the SiC rods, which was low, was avoided. (a) Resonant cavity (b) Control panel.

composed of insulation layer, aided heaters, and sample bin was shown in Figure 2. The aided heaters and insulation layers were SiC rods placed around and porous mullite plate and mullite fibers, respectively. The porous mullite plates possessed excellent thermal shock resistance and thermal insulation effect. Mullite fibers enhanced the thermal insulation effect, which not only ensured the stability of the temperature change of the samples in heating and cooling stage but also improved the heating uniformity of samples. And at the same time, the disadvantages that the temperature of samples close to the SiC rods in the insulation structure were high and the temperature away from the SiC rods, which was low, was avoided.

**2.2. Preparation of SiC/Al<sub>2</sub>O<sub>3</sub> Composite Samples.** In mullite reinforced SiC/Al<sub>2</sub>O<sub>3</sub> composites, the composition of SiC/Al<sub>2</sub>O<sub>3</sub> composite powders were 50 vol.% Al<sub>2</sub>O<sub>3</sub> and 50 vol.% SiC. The SiC/Al<sub>2</sub>O<sub>3</sub> composite powders are composed of Al<sub>2</sub>O<sub>3</sub> powders and SiC particles coated on SiO<sub>2</sub>. The morphologies of raw powders were characterized by SEM (Czech FEI Company Quanta 250). The Al<sub>2</sub>O<sub>3</sub> powders with a mean particle size less than 300 nm were commercially

purchased (Beijing Deke Daojun Technology Co., Ltd), which was shown in Figure 3. In the previous research, it was found that the SiC/Al<sub>2</sub>O<sub>3</sub> composites with the SiC particle size of 5 μm had good mechanical properties. Therefore, the SiC particle size of 5 μm was taken as the center, through the increase and decrease of SiC particle size, the influence of SiC particle size changes on the mechanical properties of SiC/Al<sub>2</sub>O<sub>3</sub> composites were studied. The SiC raw particles (Henan Haixu Abrasive Co., Ltd.) were commercially purchased and were available in four sizes, which were 1 μm, 5 μm, 50 μm, and 125 μm (Figure 4).

In order to coat SiO<sub>2</sub> on SiC particles, a sol-gel method was used [30]. Through the hydrolyzation of tetraethyl orthosilicate (TEOS), the coating process was carried out. For the sake of solving the agglomeration problem, the SiC particles were suspended in distilled water and treated with the ultrasonic for 30 min. Then, the SiC particles were evenly distributed in distilled water. By controlling the mixing ratio of TEOS and ethanol the SiO<sub>2</sub> with a volume fraction of 10% was coated on SiC particles. During the coating process, a certain amount of TEOS and ethanol were added to the suspension of SiC particles. The mixture was evenly stirred on a magnetic stirrer for 4 h. By citric acid, the pH value of

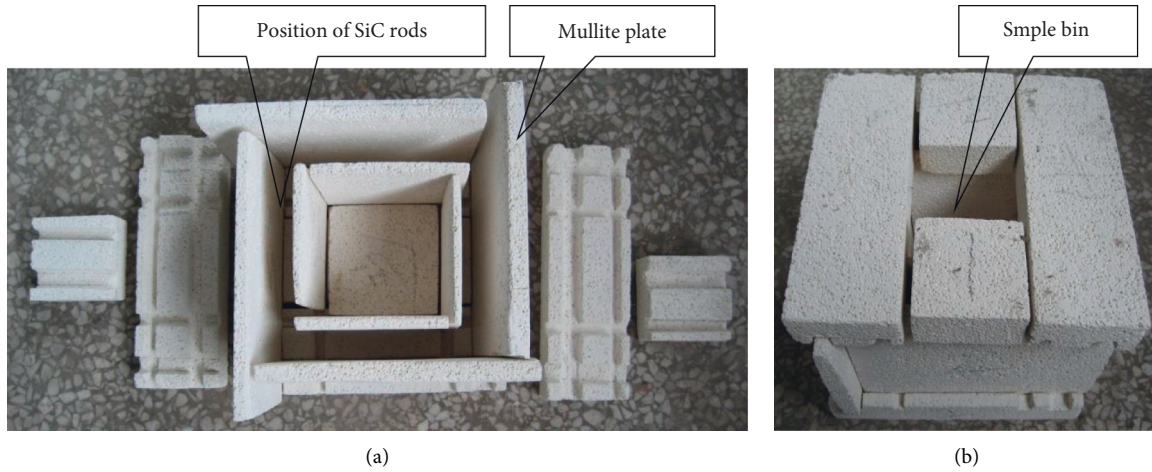


FIGURE 2: The thermal insulation based on hybrid heating mode. (a) Exploded figuer (b) Combination figuer.

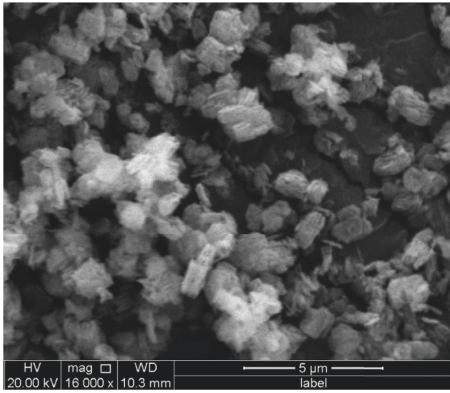


FIGURE 3: SEM image of Al<sub>2</sub>O<sub>3</sub> powders.

the suspension was firstly adjusted at about 3. Then, after the TEOS was fully hydrolyzed, the pH value of the suspension was controlled at 9 by dropping ammonia water. A few minutes later, the gel of SiC particles coated on SiO<sub>2</sub> was formed. In a blast drying oven, the gel of coated particles was dried 10 h at 80°C. Later, the coated particles were mixed with Al<sub>2</sub>O<sub>3</sub> particles. Figure 5 shows the SEM image of the SiC/Al<sub>2</sub>O<sub>3</sub> composite powders, which indicates that the Al<sub>2</sub>O<sub>3</sub> particles uniformly mix with the SiC particles coated on SiO<sub>2</sub>. In the end, through sol-gel method, the SiC/Al<sub>2</sub>O<sub>3</sub> composite powders were prepared. By the reaction between Al<sub>2</sub>O<sub>3</sub> and SiO<sub>2</sub>, the mullite was formed during microwave sintering.

Next, in a special mould (Figure 6(a)), the SiC/Al<sub>2</sub>O<sub>3</sub> composite powders were cold pressed at 3 MPa for 1 min into green compacts (Figure 6(b)). Then, the green compacts were placed in the thermal insulation structure, and sintered in the microwave furnace. By adjusting the input power, the heating rate was controlled. At the same time, the changes between the reflected power and temperature were also detected. With an approximately heating rate of 10°C/min, the green compacts were sintered at 1500°C for 30 min. After that, the samples of SiC/Al<sub>2</sub>O<sub>3</sub> composites were slowly

cooled down to room temperature in the furnace at about 15°C/min.

### 3. Experimental Process

**3.1. Bulk Density Test.** A high-precision solid-liquid electronic hydrometer (DE-120T, Shenzhen Dahong Meituo density measuring instrument Co., Ltd.) was used to measure the bulk density of SiC/Al<sub>2</sub>O<sub>3</sub> composite samples, according to the Archimedes method, with distilled water as immersion medium. The bulk density of SiC/Al<sub>2</sub>O<sub>3</sub> composite samples is calculated from the following formula:

$$\rho = \frac{m_1}{m_3 - m_2} \rho_0, \quad (1)$$

where  $\rho$  is the bulk density of sample, g/cm<sup>3</sup>.  $m_1$ ,  $m_2$ , and  $m_3$  are the dry weight, suspended weight, and wet weight of sample, respectively.  $\rho_0$  is the density of distilled water, g/cm<sup>3</sup>.

**3.2. Fracture Toughness Test.** Fracture toughness refers to the ability of a material to prevent the unstable propagation of macro cracks. It is also a toughness parameter for a material to resist brittle failure. The fracture toughness was measured by single side notched beam method (SENB), with a span of 16 mm [31, 32]. The size of the fracture toughness specimen is 2 mm × 4 mm × 22 mm, and the cross-head speed of universal material testing machine is 0.5 mm/min. The fracture toughness of SiC/Al<sub>2</sub>O<sub>3</sub> composite samples is calculated from the following formula:

$$K_{IC} = Y \frac{3PL}{2BW^2} \sqrt{a}, \quad (2)$$

where  $P$  is the breaking load of sample, N.  $L$  is the span between lower supports, 16 mm.  $B$  and  $W$  are the width and thickness of sample, 2 mm, 4 mm, respectively.  $a$  is the notch depth of sample, 0.8–1.2 mm.  $Y$  is a constant [33]. When the ratio of  $L/W$  is equal to 4 [34], the value of  $Y$  can be calculated by the following formula:



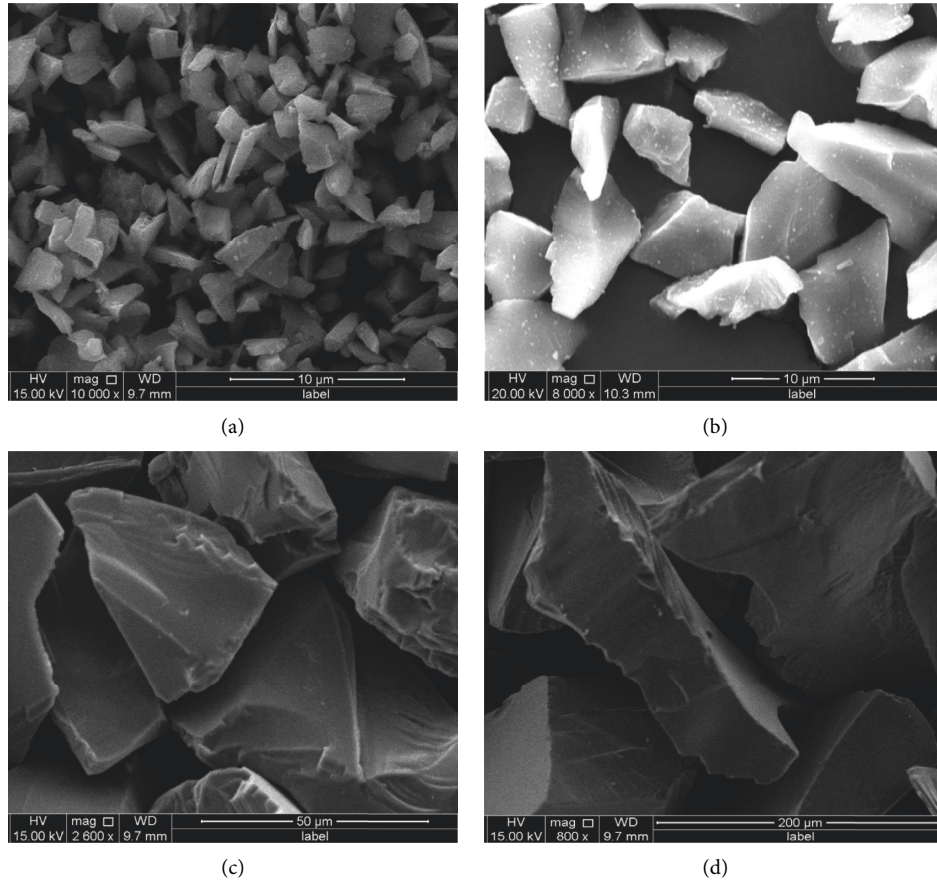


FIGURE 4: SEM images of SiC particles with different particle size. (a) SiC particles of 1 μm. (b) SiC particles of 5 μm. (c) SiC particles of 50 μm. (d) SiC particles of 125 μm.

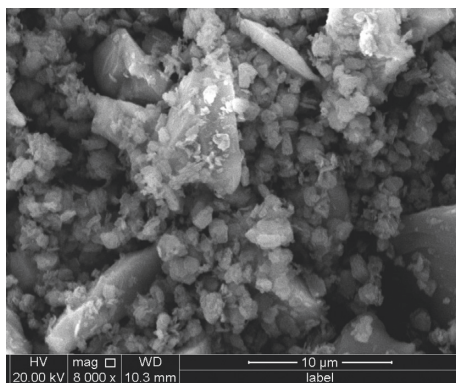


FIGURE 5: SEM image of SiC/Al<sub>2</sub>O<sub>3</sub> composite powders.

$$Y = 1.93 - 3.07 \frac{a}{W} + 14.53 \left(\frac{a}{W}\right)^2 - 25.11 \left(\frac{a}{W}\right)^3 + 25.8 \left(\frac{a}{W}\right)^4. \tag{3}$$

**3.3. Thermal Shock Resistance Test.** Thermal shock resistance refers to the ability of a material to resist damage under rapid temperature changes. The thermal shock resistance is not only one of the important properties of refractories but also

the comprehensive embodiment of mechanical and thermal properties of materials under rapid temperature changes. The thermal shock resistance of mullite reinforced SiC/Al<sub>2</sub>O<sub>3</sub> composites was studied by measuring the flexural strength retention of multiple water quenching cycles at 1000°C [35, 36]. For this purpose, the temperature of the heating furnace was raised to 1000°C. After holding for 20 min, the samples with the size of 3 mm × 4 mm × 35 mm were quickly put into the furnace. The thermal cycle process of samples was composed of heat preservation process and quench process. The heat preservation process was that the samples were put into the furnace with a temperature of 1000°C for 15 min. And the quench process was that after the heat preservation process, the samples were immediately water quenched for 5 min. This thermal cycle of heat preservation and quenching was repeated and the selected thermal shock cycles were 0, 5, 10, and 15 times, respectively. There were two main reasons for this choice. One was that according to references, the number of thermal shock cycles given in many references was 0, 5, 10, and 15 times. The other was based on the previous research. In the previous research, the thermal shock resistance cycles were 0, 5, 10, and 15 times. After the thermal shock cycle was completed, the flexural strength was tested on samples by three-point bending method (Figure 7). The three-point bending method was performed using universal testing machines



FIGURE 6: Pressing mould and green compacts of samples. (a) The special mould (b) Green compacts of SiC/Al<sub>2</sub>O<sub>3</sub> composites.

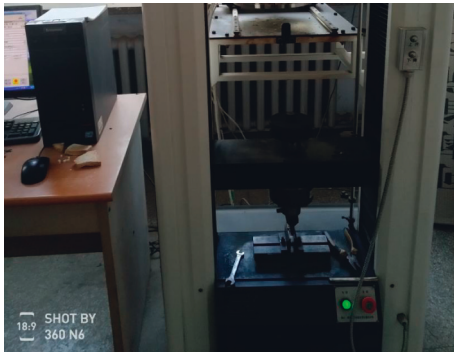


FIGURE 7: Measurement of flexural strength by three-point bending method.

(WD-P4504, Jinan Test Machine Co., Ltd.). The span and cross-head speed were 30 mm and 0.5 mm/min, respectively.

Based on the test values of flexural strength, the flexural strength retention of samples after several thermal cycles was calculated. The flexural strength retention of SiC/Al<sub>2</sub>O<sub>3</sub> composites was expressed as  $R$ . Under the condition of the same sample composition,  $R$  was defined as the ratio of the flexural strength of samples after  $n$  times of thermal shock cycles to the flexural strength of samples without thermal shock cycles. The flexural strength retention of samples can be calculated by the following formula:

$$R_n = \frac{\sigma_n}{\sigma_0} \times 100\%, \quad (4)$$

where  $R$  is the flexural strength retention.  $n$  is the number of thermal cycles.  $R_0$ ,  $R_5$ ,  $R_{10}$ , and  $R_{15}$  are the flexural strength retention of samples after 0, 5, 10, and 15 times of thermal cycles, respectively.  $\sigma_0$  is the flexural strength of samples without thermal shock cycles, and  $\sigma_n$  is the flexural strength of samples after  $n$  times of thermal shock cycles.

## 4. Experimental Results and Analysis

**4.1. Experimental Results.** The properties of mullite reinforced SiC/Al<sub>2</sub>O<sub>3</sub> composites with different SiC particle sizes are listed as Table 1.

The flexural strength of mullite reinforced SiC/Al<sub>2</sub>O<sub>3</sub> composites with different SiC particle sizes under different thermal shock cycles are listed as Table 2.

The flexural strength retention of mullite reinforced SiC/Al<sub>2</sub>O<sub>3</sub> composites with different SiC particle sizes under different thermal shock cycles are listed as Table 3.

**4.2. Analysis of Experimental Results.** As we all know, the mechanical properties of ceramic matrix composites are closely related to its microstructure. The SEM images of mullite reinforced SiC/Al<sub>2</sub>O<sub>3</sub> composites with different SiC particle sizes after microwave sintering were shown in Figure 8.

It can be clearly seen from Figure 8(a) that there were many pores in the samples of SiC (1  $\mu$ m)/Al<sub>2</sub>O<sub>3</sub> composites. The SiO<sub>2</sub> coated on SiC particles melted, but did not form a good interface with the surrounding Al<sub>2</sub>O<sub>3</sub> particles. The reason was that the selected SiC particle size (1  $\mu$ m) was too small to achieve good aggregation. The samples were mainly heated by the aided heaters of SiC rods and the self-heating cannot be well realized. Therefore, the particles grew slowly and the interface between Al<sub>2</sub>O<sub>3</sub> and SiO<sub>2</sub> was not good. With the increase of SiC particle size (5  $\mu$ m), there were few pores in the composites as shown in Figure 8(b). Through the reaction of SiO<sub>2</sub> and Al<sub>2</sub>O<sub>3</sub> particles, the mullite whiskers with large length diameter ratio had been formed and presented a bridge structure through the pores. As a result, the bridging mullite whiskers improve the interface between SiC and Al<sub>2</sub>O<sub>3</sub> particles. As can be seen from Figure 8(c), with the continuous increase of SiC particle size (50  $\mu$ m) in samples, although the mullite whiskers still existed after microwave sintering, its length diameter ration was small. And there were many pores in SiC (50  $\mu$ m)/Al<sub>2</sub>O<sub>3</sub> composites. Due to the large size (50  $\mu$ m) of SiC particles, the samples can quickly achieve thermal aggregation during microwave sintering, while the rapid outward diffusion of heat cannot be realized, resulting in the formation of many pores. With the further increase of SiC particle size (125  $\mu$ m), the mullite whiskers with large length diameter ratio did not form after microwave sintering, as shown in Figure 8(d). The morphology of mullite phase in samples is short rod-like.

TABLE 1: Properties of samples with different SiC particle sizes.

Composites	Bulk density, $\rho$ (g/cm <sup>3</sup> )	Fracture toughness, $K_{IC}$ (MPa·m <sup>1/2</sup> )	Flexural strength, $\sigma_0$ (MPa)
SiC (1 $\mu$ m)/Al <sub>2</sub> O <sub>3</sub>	1.76	1.04	30
SiC (5 $\mu$ m)/Al <sub>2</sub> O <sub>3</sub>	2.06	1.98	63
SiC (50 $\mu$ m)/Al <sub>2</sub> O <sub>3</sub>	1.94	1.12	34
SiC (125 $\mu$ m)/Al <sub>2</sub> O <sub>3</sub>	1.88	0.93	29

TABLE 2: Flexural strength of samples under different thermal shock cycles.

Composites	Flexural strength, $\sigma_0$ /MPa 0 times	Flexural strength, $\sigma_5$ /MPa 5 times	Flexural strength, $\sigma_{10}$ /MPa 10 times	Flexural strength, $\sigma_{15}$ /MPa 15 times
SiC (1 $\mu$ m)/Al <sub>2</sub> O <sub>3</sub>	30	16	7	6
SiC (5 $\mu$ m)/Al <sub>2</sub> O <sub>3</sub>	63	38	19	17
SiC (50 $\mu$ m)/Al <sub>2</sub> O <sub>3</sub>	34	19	10	9
SiC (125 $\mu$ m)/Al <sub>2</sub> O <sub>3</sub>	29	14	8	7

TABLE 3: Flexural strength retention of samples under different thermal shock cycles.

Composites	Flexural strength retention, $R_0$ /%	Flexural strength retention, $R_5$ /%	Flexural strength retention, $R_{10}$ /%	Flexural strength retention, $R_{15}$ /%
SiC (1 $\mu$ m)/Al <sub>2</sub> O <sub>3</sub>	100	53	23	20
SiC (5 $\mu$ m)/Al <sub>2</sub> O <sub>3</sub>	100	60	30	27
SiC (50 $\mu$ m)/Al <sub>2</sub> O <sub>3</sub>	100	56	29	26
SiC (125 $\mu$ m)/Al <sub>2</sub> O <sub>3</sub>	100	48	28	24

There were also many pores in SiC (125  $\mu$ m)/Al<sub>2</sub>O<sub>3</sub> composites. Due to the large SiC particle size (125  $\mu$ m) and rapid temperature rise of samples, the Al<sub>2</sub>O<sub>3</sub> particles and SiO<sub>2</sub> cannot react fully, so, the mullite grains formed had no time to grow. Under the condition of gas-solid two-phase co-existence, the anisotropic growth of mullite grains was limited to a certain extent [37], and the growth rate in all directions was relatively fast, making the mullite phase formed in a short rod-like shape.

The curve of bulk density of mullite reinforced SiC/Al<sub>2</sub>O<sub>3</sub> composites with SiC particle size was shown in Figure 9.

It can be observed from Figure 9 that the density of SiC (1  $\mu$ m)/Al<sub>2</sub>O<sub>3</sub> composites after microwave sintering was relatively small. With the increase of SiC particle size in samples, the bulk density of SiC/Al<sub>2</sub>O<sub>3</sub> composites also increased. The bulk density of SiC (5  $\mu$ m)/Al<sub>2</sub>O<sub>3</sub> composites reached the maximum. The reason was that with the increase of SiC particle size, the better thermal aggregation on the particle surface can be realized. The SiO<sub>2</sub> in samples was melted at high temperature to form a flowing glass phase and fill the pores, so that the porosity of samples was reduced and the density was improved. With the continuous increase of SiC particle size in samples, the bulk density of samples after sintering decreased (Figure 9). The bulk density of SiC (50  $\mu$ m)/Al<sub>2</sub>O<sub>3</sub> composites was lower than that of SiC (5  $\mu$ m)/Al<sub>2</sub>O<sub>3</sub> composites after microwave sintering, and the bulk density of SiC (125  $\mu$ m)/Al<sub>2</sub>O<sub>3</sub> composites decreased further after microwave sintering. Combined with the analysis results of SEM images in Figure 8, the reason for this phenomenon was that the SiC particle size in samples was

too large, the heating rate was too fast, and large amounts of heat accumulated on the particle surface. As a result, the rapid outward diffusion of heat cannot be realized, and the pores formed during the sintering process. Therefore, the porosity of samples was increased, the structure was loose and the bulk density was low. For the bulk density of samples, the reason was the thermal aggregation on the SiC particles. If the thermal aggregation was poor or the thermal aggregation cannot be released in time, the bulk density of SiC/Al<sub>2</sub>O<sub>3</sub> composite was relatively low. Overall, with the increase of SiC particle size, the bulk density of SiC/Al<sub>2</sub>O<sub>3</sub> composites increased first and then, decreased.

The curve of fracture toughness of mullite reinforced SiC/Al<sub>2</sub>O<sub>3</sub> composites with SiC particle size shown in Figure 10.

From Figure 10, it can be seen that the fracture toughness of SiC (1  $\mu$ m)/Al<sub>2</sub>O<sub>3</sub> composites was relatively low. With the increase of SiC particle size dispersed in samples, the fracture toughness increased. When the SiC particle size increased to about 5  $\mu$ m, the fracture toughness of SiC (5  $\mu$ m)/Al<sub>2</sub>O<sub>3</sub> composites reached the maximum 1.98 MPa·m<sup>1/2</sup>. This is because the content of mullite whiskers was relatively high, and the mullite whisker connecting phase was formed between the particles, which improved the fracture toughness of the samples. However, when the SiC particle size dispersed in the samples continued to increase, the fracture toughness of SiC (50  $\mu$ m)/Al<sub>2</sub>O<sub>3</sub> composites and SiC (125  $\mu$ m)/Al<sub>2</sub>O<sub>3</sub> composites both decreased. The main reason for this phenomenon was that although the mullite was also formed in SiC (50  $\mu$ m)/Al<sub>2</sub>O<sub>3</sub> composites at high temperature, the growth power of mullite was not enough,



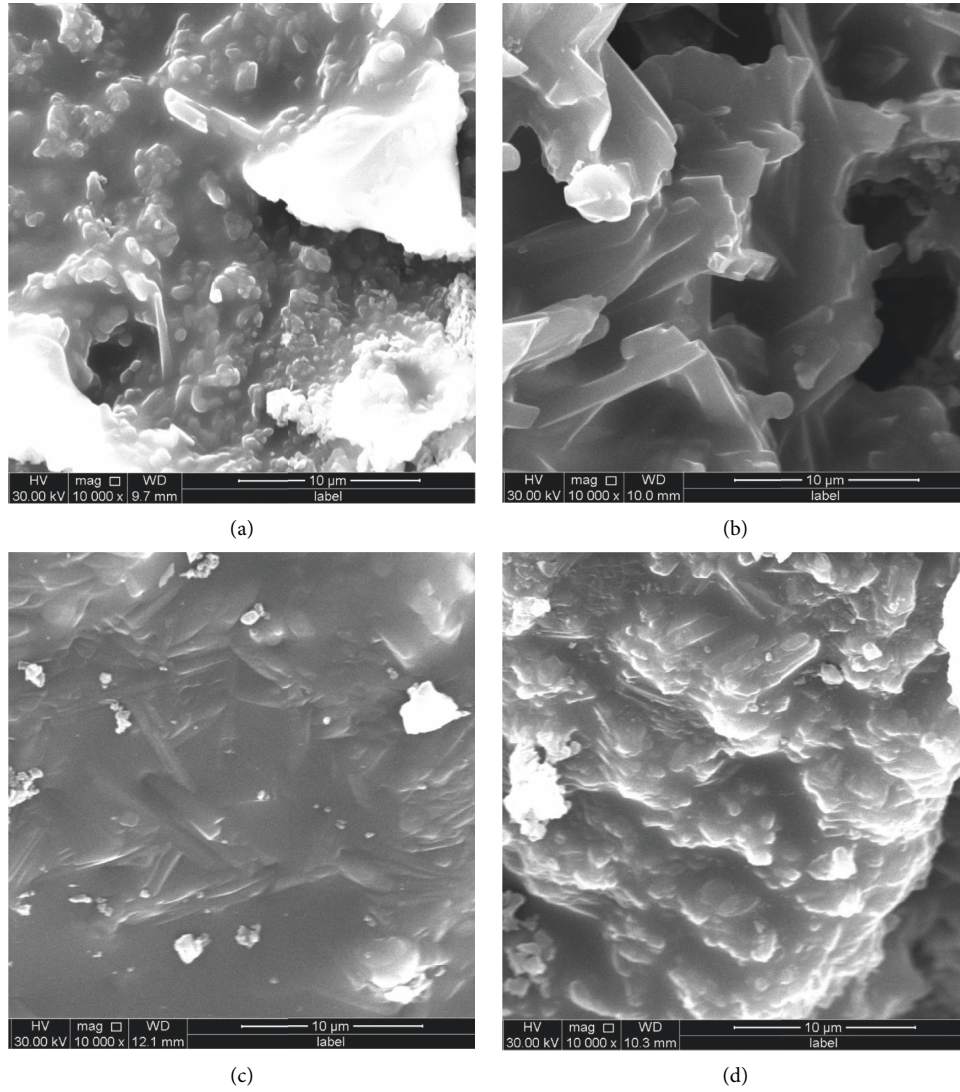


FIGURE 8: SEM images of mullite reinforced SiC/Al<sub>2</sub>O<sub>3</sub> composites with different SiC particle sizes. (a) Samples of SiC(1 μm)/Al<sub>2</sub>O<sub>3</sub> composites. (b) Samples of SiC(5 μm)/Al<sub>2</sub>O<sub>3</sub> composites. (c) Samples of SiC(50 μm)/Al<sub>2</sub>O<sub>3</sub> composites. (d) Samples of SiC(125 μm)/Al<sub>2</sub>O<sub>3</sub> composites.

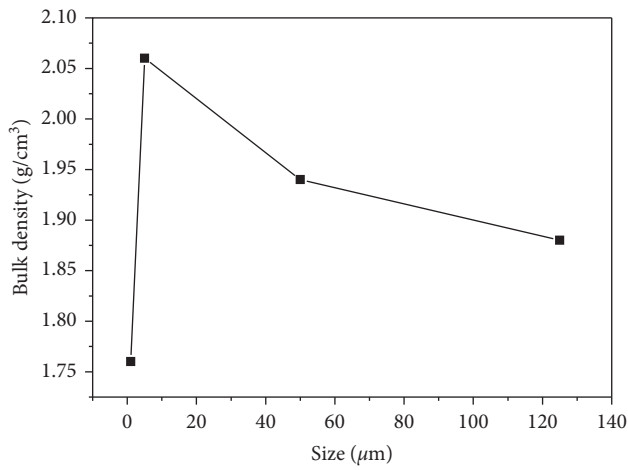


FIGURE 9: Curve of bulk density of samples with SiC particle size.

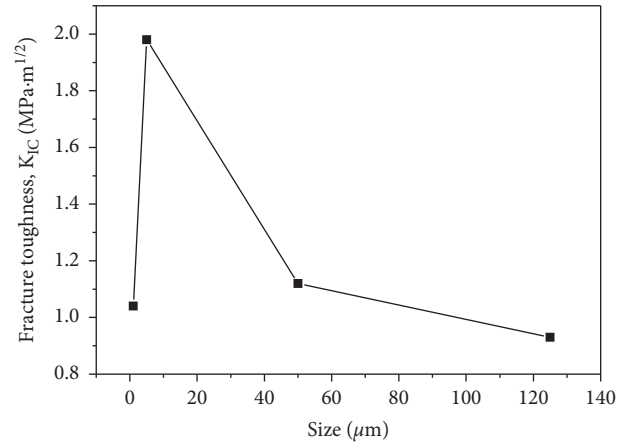


FIGURE 10: Curve of fracture toughness of samples with SiC particle size.



so the mullite whiskers with large length diameter ratio did not form, while the morphology of mullite in SiC (125  $\mu\text{m}$ )/Al<sub>2</sub>O<sub>3</sub> composites after microwave sintering was short rod-like and the short rod-like mullite was basically no aspect ratio. Therefore, the mullite whiskers bridging between particles were not formed in SiC (50  $\mu\text{m}$ )/Al<sub>2</sub>O<sub>3</sub> composites and SiC (125  $\mu\text{m}$ )/Al<sub>2</sub>O<sub>3</sub> composites, so the fracture toughness of these samples was not high. For the fracture toughness, the reason was the formation of mullite whiskers. If there were mullite whiskers with large length diameter ratio, the flexural strength and fracture toughness of samples were high. With the increase of SiC particle size, the fracture toughness of SiC/Al<sub>2</sub>O<sub>3</sub> composites also increased first and then decreased.

The curves of flexural strength of mullite reinforced SiC/Al<sub>2</sub>O<sub>3</sub> composites with different SiC particle size after 0, 5, 10, and 15 times of thermal cycles were shown in Figure 11. Figure 11 shows the thermal shock resistance of SiC/Al<sub>2</sub>O<sub>3</sub> composites.

According to Figure 11, when the four groups of samples were not subjected to thermal shock, the flexural strength of SiC/Al<sub>2</sub>O<sub>3</sub> composites increased with the increase of SiC particle size dispersed in the samples. The flexural strength of SiC (5  $\mu\text{m}$ )/Al<sub>2</sub>O<sub>3</sub> composites reached the maximum value of 63 MPa. This is mainly due to the synthesis amount of mullite whiskers increased with the increase of SiC particle size, which enhanced the flexural strength of the samples. When the SiC particle size in SiC/Al<sub>2</sub>O<sub>3</sub> composites further increased, the flexural strength of samples decreased. The main reason is that when the added SiC particle size was too large (50  $\mu\text{m}$  and 150  $\mu\text{m}$ ), the temperature rise of samples was too fast, Al<sub>2</sub>O<sub>3</sub> and SiO<sub>2</sub> cannot fully react, and the mullite grains had no time to grow, which reduced the flexural strength of SiC/Al<sub>2</sub>O<sub>3</sub> composites. In short, with the increase of SiC particle size, the flexural strength of SiC/Al<sub>2</sub>O<sub>3</sub> composites also increased first and then decreased. After 5 times of thermal shock cycles, the flexural strength retention of SiC (125  $\mu\text{m}$ )/Al<sub>2</sub>O<sub>3</sub> composites was only 48%, and the flexural strength retentions of SiC (1  $\mu\text{m}$ )/Al<sub>2</sub>O<sub>3</sub> composites, SiC (5  $\mu\text{m}$ )/Al<sub>2</sub>O<sub>3</sub> composites and SiC (50  $\mu\text{m}$ )/Al<sub>2</sub>O<sub>3</sub> composites were 53%, 60%, and 56%, respectively. After 15 times of thermal shock cycles, the flexural strength retention of SiC (1  $\mu\text{m}$ )/Al<sub>2</sub>O<sub>3</sub> composites was 20% and the flexural strength retention of SiC (125  $\mu\text{m}$ )/Al<sub>2</sub>O<sub>3</sub> composites was 26%. While, the flexural strength retention of SiC (5  $\mu\text{m}$ )/Al<sub>2</sub>O<sub>3</sub> composites was 27%. Although, the flexural strength retention of SiC (50  $\mu\text{m}$ )/Al<sub>2</sub>O<sub>3</sub> composites was very similar to that of the SiC (5  $\mu\text{m}$ )/Al<sub>2</sub>O<sub>3</sub> composites (Table 3), their flexural strength was greatly different. Therefore, the thermal shock resistance of SiC (50  $\mu\text{m}$ )/Al<sub>2</sub>O<sub>3</sub> composites was not very good. With the increase of thermal shock cycles, the flexural strength of four groups of SiC/Al<sub>2</sub>O<sub>3</sub> composites all decreased. After 5 thermal cycles, the flexural strength of four groups of SiC/Al<sub>2</sub>O<sub>3</sub> composites decreased sharply. As the continued increase of thermal shock cycles, the flexural strength of four groups of SiC/Al<sub>2</sub>O<sub>3</sub> composites decreased gently. Comparing the above four groups of samples, the SiC (5  $\mu\text{m}$ )/Al<sub>2</sub>O<sub>3</sub> composites had good thermal shock resistance. Better thermal shock

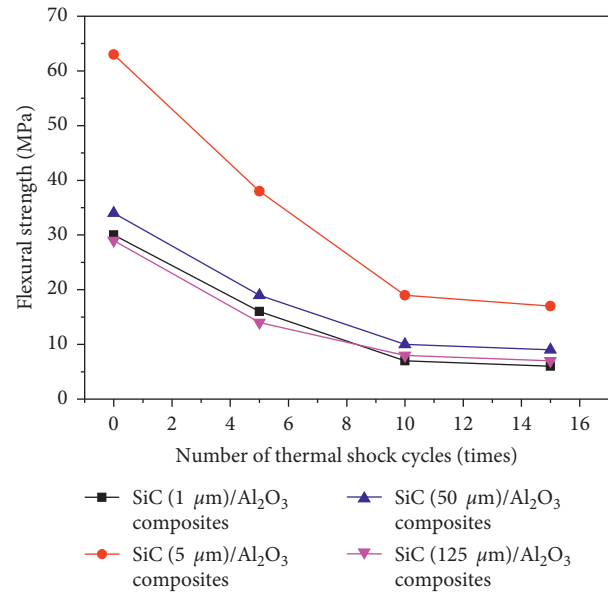


FIGURE 11: Curve of flexural strength of samples with different SiC particle size after several thermal cycles.

resistance of mullite reinforced SiC/Al<sub>2</sub>O<sub>3</sub> composites obtained by microwave sintering can be applied to the refractory and heat insulation materials.

Based on the above analysis of microstructure, bulk density, and thermal shock resistance, among the four groups of SiC/Al<sub>2</sub>O<sub>3</sub> composites (SiC particle size of 1  $\mu\text{m}$ , 5  $\mu\text{m}$ , 50  $\mu\text{m}$ , and 125  $\mu\text{m}$ ), the SiC (5  $\mu\text{m}$ )/Al<sub>2</sub>O<sub>3</sub> composites possessed the best comprehensive mechanical properties.

## 5. Mechanism Analysis of Microwave Sintering

Through analyzing the microstructure and mechanical properties of SiC/Al<sub>2</sub>O<sub>3</sub> composites, it can be seen that the morphology of mullite phase was different in different group of samples. The mullite phase was mullite whisker with large length diameter ratio in SiC (5  $\mu\text{m}$ )/Al<sub>2</sub>O<sub>3</sub> composites. While, the mullite phase was short rod-like in SiC (1  $\mu\text{m}$ )/Al<sub>2</sub>O<sub>3</sub> composites, SiC (50  $\mu\text{m}$ )/Al<sub>2</sub>O<sub>3</sub> composites, and SiC (125  $\mu\text{m}$ )/Al<sub>2</sub>O<sub>3</sub> composites. It is the morphology of mullite phase that affected the mechanical properties of SiC/Al<sub>2</sub>O<sub>3</sub> composites. Through the whisker pullout and whisker bridging, the mullite whiskers toughen the SiC/Al<sub>2</sub>O<sub>3</sub> composites. During the fracture process, the whiskers were pulled out and made bridging cracks, so the cracks can be deflected and energy can be absorbed, resulting in the improvement of mechanical properties for SiC/Al<sub>2</sub>O<sub>3</sub> composites [38]. In addition to in situ mullite whiskers, the mullite whiskers can also be added externally. But there were some problems with the external mullite whiskers, such as uneven distribution, poor dispersion, difficult sintering, and poor compatibility, with interface and harmful to human body. Compared with the external whisker addition, the situ synthesized mullite whiskers in SiC/Al<sub>2</sub>O<sub>3</sub> composites can more effectively toughen the samples because of low cost, better dispersion, and without pollution[39]. For the

formation of mullite whiskers, there existed two mechanisms during the microwave sintering.

One of the reasons for the different morphology of mullite phase was the size coupling effect in microwave sintering. In the initial stage of microwave heating, the temperature rise of SiC/Al<sub>2</sub>O<sub>3</sub> composites mainly depended on the local thermal aggregation generated by the coupling of SiC particles and microwave field. When the size of SiC particles dispersed in samples was too small, such as 1 μm, the ability of SiC particles absorbing microwave loss was lower than the ability of particle surface heat diffusion. The good thermal aggregation on the surface of SiC particles cannot be achieved, resulting in slow temperature rise of samples, so the synthesis ability of mullite was limited. When the size of SiC particles dispersed in samples was too large, such as 50 μm and 125 μm, the ability of SiC particles absorbing microwave loss was higher than the ability of particle surface heat diffusion. Although the thermal aggregation on the surface of SiC particles was more, the heat cannot be diffused rapidly, resulting in the slow temperature rise of samples. The more thermal aggregation can promote the reaction of SiO<sub>2</sub> coated on SiC particles and Al<sub>2</sub>O<sub>3</sub> to synthesize mullite, but the anisotropic growth of mullite was not obvious [40], and the length and diameter of mullite whiskers were small. In the process of microwave sintering, the ability of SiC particles absorbing microwave loss and the ability of SiC particle surface heat diffusion needed to be balanced so that the mullite grains can grow rapidly along the one-dimensional direction into whiskers with large length diameter ratio. Therefore, there was a critical size (about 5 μm) of SiC particles. When the size of SiC particles dispersed in samples was within the critical size range, the size coupling effect was the most obvious. So, the ability of SiC particles absorbing microwave loss was basically consistent with the ability of particle surface heat diffusion, which made the samples heat up rapidly at low temperature and obtained the mullite whiskers with large length and diameter and bridging between particles.

Another reason for the formation of mullite whiskers during microwave sintering was the local thermal aggregation effect. Because microwave sintering is an integral heating method, this sintering mechanism is a unique feature of microwave sintering. In the conventional sintering method, materials absorbed energy and heated up by means of conduction, convection, and thermal radiation. The sintering mechanism of microwave sintering was completely different from that of conventional sintering. So, in the conventional sintering process, there were no size coupling effect and local thermal aggregation effect. The schematic of mullite growth during microwave sintering and conventional sintering was shown in Figure 12. It can be seen that the mullite growth is different during the two sintering methods [7].

Figure 12(a) shows the growth process of mullite crystal in microwave field. When the SiC/Al<sub>2</sub>O<sub>3</sub> composites were prepared by microwave sintering, due to the high SiC dielectric loss, the SiC rods (aided heaters) in the thermal insulation structure absorbed the microwave

energy to generate heat and transfer the heat from outside to inside. At the same time, the SiC particles in samples also preferentially absorbed the microwave energy to make the local instantaneous temperature rise on the SiC particle surface, causing local thermal aggregation effect, and the generated local heat diffused from inside to outside. The local thermal aggregation heated the SiO<sub>2</sub> coated on SiC particles to form a molten of glass phase, which reacted with Al<sub>2</sub>O<sub>3</sub> to form mullite. During sintering process, the microwave hybrid heating produced two forms of heat. With the continuous increase of microwave input power, the local thermal aggregation effect was strengthened, which promoted the anisotropic growth of mullite grains, made the mullite grains grew rapidly along one-dimensional direction, and formed the mullite whiskers with large length diameter ratio.

Figure 12(b) shows the growth process of mullite crystal in conventional sintering process. In conventional sintering of SiC/Al<sub>2</sub>O<sub>3</sub> composites, the samples are mainly heated by thermal radiation and heat conduction of conventional furnace. The heat was transferred from outside to inside and cannot form the local thermal aggregation effect to make the surface of SiC particles temperature rise instantaneously. This heating method raises the temperature slowly, and the energy dissipates greatly from outside to inside, which causes the less energy use for the synthesis of mullite. Therefore, the growth rate of mullite grains is slow and the anisotropic growth of mullite is not obvious, resulting in the formation of mullite phase with small length diameter ratio.

The SEM images of SiC/Al<sub>2</sub>O<sub>3</sub> composites sintered by microwave sintering and conventional sintering were shown in Figure 13.

It can be obviously seen that the morphology of mullite phase in Figure 13(a) is different from Figure 13(b). Compared with the conventional sintering, the greatest advantage of microwave sintering is the local thermal aggregation effect. Because of the thermal aggregation effect, the mullite whiskers formed around the SiC particles. The bridging mullite whiskers with large length diameter ratio only existed in samples prepared by microwave sintering. As shown in Figure 13(b), the SiO<sub>2</sub> coated on SiC particles only melted and reacted with Al<sub>2</sub>O<sub>3</sub> to form mullite, but the morphology of mullite was not whiskered. The reason is that the anisotropic growth of mullite is not promoted during conventional sintering. Therefore, the mullite whiskers with large length diameter ratio were not formed.

Due to the different sintering mechanism, the morphologies of mullite phase are different in different sintering methods, resulting in different mechanical properties. The main reasons are the size coupling effect and thermal aggregation effect analyzed above. In addition, compared with the conventional sintering, the microwave sintering can reduce the synthesis temperature of mullite, resulting in energy savings. Moreover, microwave sintering is also a relatively clean, pollution-free, and waste gas free sintering method [41]. Therefore, microwave sintering is a kind of green manufacturing with great potential.

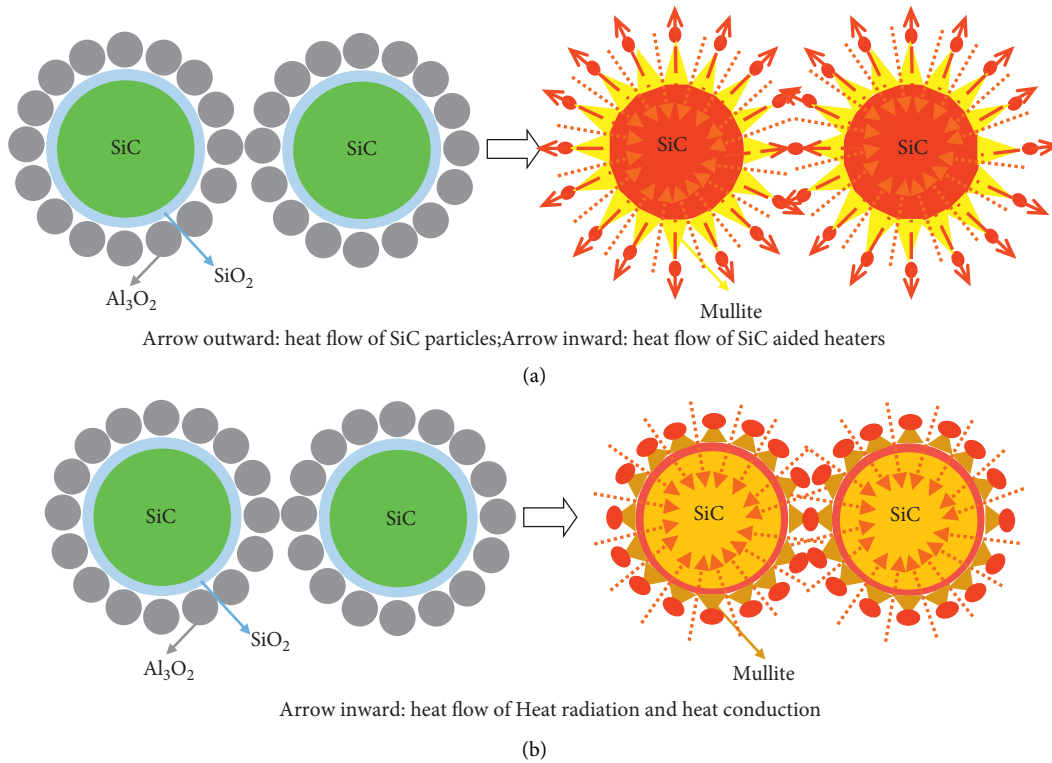


FIGURE 12: Schematic of mullite growth during microwave sintering and conventional sintering. (a) Microwave sintering. (b) Conventional sintering.

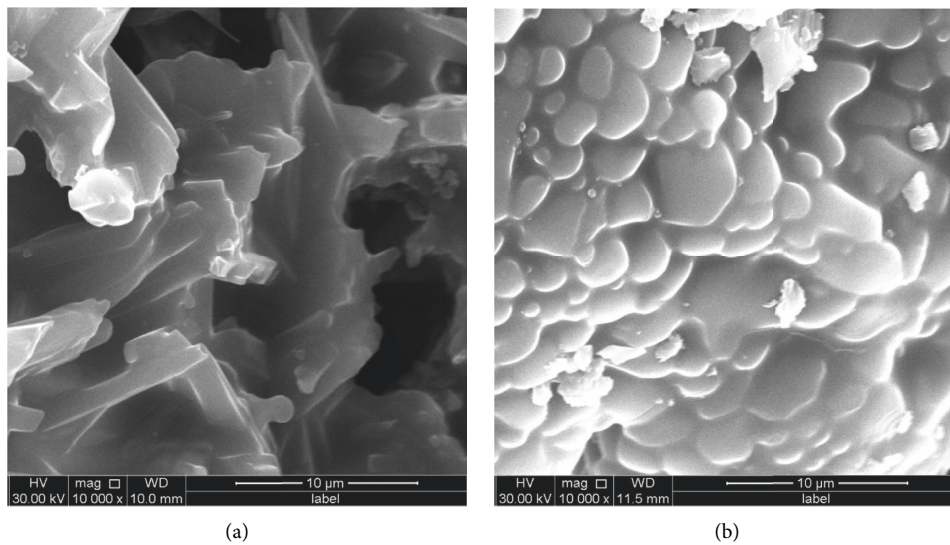


FIGURE 13: SEM images of SiC/Al<sub>2</sub>O<sub>3</sub> composites sintered by microwave sintering and conventional sintering (a) Samples of microwave sintering (b) Samples of conventional sintering.

## 6. Conclusion

(1) Through microwave sintering, the in situ synthesized mullite reinforced SiC/Al<sub>2</sub>O<sub>3</sub> composites with different SiC particle size were prepared. The composite powders of samples were composed of SiC particles, coated with SiO<sub>2</sub> by a sol-gel method and Al<sub>2</sub>O<sub>3</sub> particles. During microwave sintering, the bridging

mullite whiskers with large length diameter ratio were found in the SiC (5 μm)/Al<sub>2</sub>O<sub>3</sub> composites.

(2) With the increase of SiC particle size in samples, the bulk density of SiC/Al<sub>2</sub>O<sub>3</sub> composites first increased and then decreased. The bulk density of SiC (5 μm)/Al<sub>2</sub>O<sub>3</sub> composites was higher than that of other SiC/Al<sub>2</sub>O<sub>3</sub> composites, which reached the maximum value 2.06 g/cm<sup>3</sup>.



- (3) With the increase of SiC particle size in samples, the fracture toughness and flexural strength of SiC/Al<sub>2</sub>O<sub>3</sub> composites also first increased and then decreased. The fracture toughness and flexural strength of SiC (5 μm)/Al<sub>2</sub>O<sub>3</sub> composites were higher than those of other SiC/Al<sub>2</sub>O<sub>3</sub> composites, which reached the maximum value 1.98 MPa·m<sup>1/2</sup> and 63 MPa, respectively.
- (4) With the increase of thermal shock cycles, the flexural strength retention of SiC/Al<sub>2</sub>O<sub>3</sub> composites with different SiC particle size also decreased. Among the four groups of SiC/Al<sub>2</sub>O<sub>3</sub> composites, the flexural strength retention of SiC (5 μm)/Al<sub>2</sub>O<sub>3</sub> composites was also higher than those of other SiC/Al<sub>2</sub>O<sub>3</sub> composites. After 5, 10, and 15 times of thermal shock cycles, the flexural strength retention of SiC (5 μm)/Al<sub>2</sub>O<sub>3</sub> composites were 38%, 19%, and 17%, respectively, which indicated the better thermal shock resistance.
- (5) The morphology of mullite phase were mullite whiskers in SiC (5 μm)/Al<sub>2</sub>O<sub>3</sub> composites, which was due to the size coupling effect and thermal aggregation effect in microwave sintering. Based on the size coupling effect and thermal aggregation effect, the anisotropic growth of mullite grains in SiC (5 μm)/Al<sub>2</sub>O<sub>3</sub> composites was promoted and the mullite grains grew rapidly along one-dimensional direction during microwave sintering, while the sintering mechanism was heat radiation and heat transfer during conventional sintering, resulting in mullite phase with weak anisotropic growth.

Due to the unique sintering mechanism, the microwave sintering preserves the characteristics of fast speed, clean, and pollution-free, which brings the results of energy savings and environment-friendly. Therefore, microwave sintering is a kind of advanced material preparation process based on green manufacturing.

## Data Availability

The data used to support the findings of this study are included within the article.

## Conflicts of Interest

The authors declare that they have no conflicts of interest.

## Acknowledgments

The authors gratefully acknowledge the financial support from the Science and Technology Project of Henan Province for Tackling Key Problems (182102210030).

## References

- [1] X. U. Ni, "Research on manufacturing process and technology of chemical equipment based on the concept of green manufacturing," *Process technology*, no. 15, pp. 236–237, 2020.
- [2] C. Hu, G. Gui, S. Xie, and G. Y. Xiao, "Implementing method of green manufacture oriented material, energy and environment," *Coal Mine Machinery*, vol. 28, no. 3, pp. 107–109, 2007.
- [3] C. Wu, "Analysis of green manufacturing technology in mechanical manufacturing process," *Internal Combustion Engines and Accessories*, no. 3, pp. 150–151, 2021.
- [4] J. Liu, N. Xiao, and L. Zhang, "New mechanical manufacturing technology of green manufacturing," *Internal Combustion Engines and Accessories*, no. 22, pp. 104–106, 2020.
- [5] J. XI, "Research on materials selection for green manufacturing," *Materials Reports*, vol. 23, no. 5, pp. 94–97, 2009.
- [6] S. Fang, *Preparation and Investigation of Mullite Lightweight thermal Insulation Materials by Microwave sintering*, Zhengzhou University (Zhengzhou), Zhengzhou, 2020.
- [7] K. Guan, *Study of the Processing and Mechanisms of Mullite Reinforced Al<sub>2</sub>O<sub>3</sub>-SiC Composites by Microwave synthesis*, Zhengzhou University (Zhengzhou), Zhengzhou, 2016.
- [8] Liu. Jin, B. Liang, J. Zhang, and Y. Ai, "Research progress on microwave dielectric ceramics prepared via microwave sintering," *Materials Reports*, vol. 36, no. 3, pp. 1–10, 2022.
- [9] H. Zhang, Y. Zhang, B. Wang, and Yang, "Preparation and characterization of continuous alumina based fiber reinforced with orientated mullite whisker," *Chemical Engineering Journal*, vol. 268, pp. 109–115, 2015.
- [10] B. Meng and J. Peng, "Effects of in situ synthesized mullite whiskers on flexural strength and fracture toughness of corundum-mullite refractory materials," *Ceramics International*, vol. 39, no. 2, pp. 1525–1531, 2013.
- [11] O. Ertugrul, R. Dalmis, S. Akpınar, I. M. Kusoglu, and Celik, "Influence of zircon particle size on conventional and microwave assisted reaction sintering of in-situ mullite-zirconia composites," *Ceramics International*, vol. 42, no. 9, pp. 11104–11117, 2016.
- [12] Q. Dang, Y. Ge, and Y. Gao, "Dynamic mechanical properties of Al<sub>2</sub>O<sub>3</sub>/SiC composite ceramic subjected to impact loading," *Acta Armamentarii*, vol. 43, no. 1, pp. 175–180, 2022.
- [13] B. Fan, W. Li, B. Dai, K. Guan, R. Zhang, and H. Li, "Preparation of mullite whiskers reinforced SiC/Al<sub>2</sub>O<sub>3</sub> composites by microwave sintering," *Processing and Application of Ceramics*, vol. 10, no. 4, pp. 243–248, 2016.
- [14] X. Dang, M. Wei, R. Zhang et al., "Crucial effect of SiC particles on in situ synthesized mullite whisker reinforced Al<sub>2</sub>O<sub>3</sub>-SiC composite during microwave sintering," *Processing and Application of Ceramics*, vol. 11, no. 2, pp. 106–112, 2017.
- [15] C. Lu, *Study on Gelcasting Process of SiC Whisker Toughened Alumina Ceramics*, Shenyang University of Technology (Shenyang), Shenyang, 2021.
- [16] S. Zhang, Y. Feng, X. Gao, Y. Song, F. Wang, and S. Zhang, "Modeling of fatigue failure for SiC/SiC ceramic matrix composites at elevated temperatures and multi-scale experimental validation," *Journal of the European Ceramic Society*, vol. 42, no. 8, pp. 3395–3403, 2022.
- [17] S. Wu and N. Claussen, "Reaction bonding and mechanical properties of mullite/silicon carbide composites," *Journal of the American Ceramic Society*, vol. 77, no. 11, pp. 2898–2904, 2010.
- [18] W. Wang, C. Zhou, G. Liu, and G. Qiao, "Molten salt synthesis of mullite whiskers on the surface of SiC ceramics," *Journal of Alloys and Compounds*, vol. 582, no. 1, pp. 96–100, 2014.

- [19] N. M. Rendtorff, L. B. Garrido, and E. F. Aglietti, "Thermal shock behavior of dense mullite-zirconia composites obtained by two processing routes," *Ceramics International*, vol. 34, no. 8, pp. 2017–2024, 2008.
- [20] X. Pian, B. Fan, H. Chen, B. Zhao, X. Zhang, and R. Zhang, "Preparation of m-ZrO<sub>2</sub> compacts by microwave sintering," *Ceramics International*, vol. 40, no. 7, pp. 10483–10488, 2014.
- [21] D. Żymełka, S. Saunier, D. Goeriot, and J. Molimard, "Densification and thermal gradient evolution of alumina during microwave sintering at 2.45GHz," *Ceramics International*, vol. 39, no. 3, pp. 3269–3277, 2013.
- [22] J. Croquesel, D. Bouvard, J. M. Chaix, C. P. Carry, S. Saunier, and S. Marinel, "Direct microwave sintering of pure alumina in a single mode cavity: grain size and phase transformation effects," *Acta Materialia*, vol. 116, pp. 53–62, 2016.
- [23] M. Xie, J. Shi, G. Chen, and X. Li, "Research progress and prospect of microwave sintering technology," *Powder Metallurgy Industry*, vol. 29, no. 3, pp. 66–72, 2019.
- [24] Z. Yin, J. Yuan, Y. Cheng, and Z. h. Wang, "Research Status of processes and mechanisms of ceramic materials by microwave sintering," *Bulletin of the Chinese Ceramic Society*, vol. 35, no. 5, pp. 1492–1497, 2016.
- [25] D. Xu, C. Fang, Y. Zhan et al., "Effect of two-step microwave sintering on the fracture toughness of alumina ceramics," *Journal of Ceramics*, vol. 39, no. 2, pp. 174–180, 2018.
- [26] H. Yang, X. Zhou, J. Yu, H. Wang, and Z. Huang, "Microwave and conventional sintering of SiC/SiC composites: flexural properties and microstructures," *Ceramics International*, vol. 41, no. 9, pp. 11651–11654, 2015.
- [27] B. Li, L. Xin, J. Cui et al., "Research process in preparation of glass ceramics by microwave sintering," *Materials Reports*, vol. 33, no. Z2, pp. 189–197, 2019.
- [28] S. Bodhak, S. Bose, and A. Bandyopadhyay, "Densification study and mechanical properties of microwave-sintered mullite and mullite-zirconia composites," *Journal of the American Ceramic Society*, vol. 94, no. 1, pp. 146–155, 2011.
- [29] R. Zhang, B. Fan, F. Zhang et al., *Special auxiliary heating and heat preservation device for microwave sintering of oxide composites*, 2012.
- [30] R. Zhang, B. Fan, F. Zhang et al., *A preparation method of mullite reinforced Al<sub>2</sub>O<sub>3</sub>/SiC composites*, vol. 9, 2015.
- [31] R. Belli, M. Wendler, J. Zorzini, L. H. da Silva, A. Petschelt, and U. Lohbauer, "Fracture toughness mode mixity at the connectors of monolithic 3Y-TZP and LS2 dental bridge constructs," *Journal of the European Ceramic Society*, vol. 35, no. 13, pp. 3701–3711, 2015.
- [32] X. Wang and A. A. Atkinson, "On the measurement of ceramic fracture toughness using single edge notched beams," *Journal of the European Ceramic Society*, vol. 35, no. 13, pp. 3713–3720, 2015.
- [33] J. Wan, M. Zhou, X. S. Yang et al., "Fracture characteristics of freestanding 8wt% Y<sub>2</sub>O<sub>3</sub>-ZrO<sub>2</sub> coatings by single edge notched beam and Vickers indentation tests," *Materials Science and Engineering A*, vol. 581, no. 5, pp. 140–144, 2013.
- [34] W. F. Brown and J. E. Srawley, *Plane Strain Crack Toughness Testing of High Strength Metallic Materials*, American Society for Testing Materials, Philadelphia, 1966.
- [35] P. Kumar, M. Nath, and A. Ghosh, "Enhancement of thermal shock resistance of reaction sintered mullite-zirconia composites in the presence of lanthanum oxide," *Materials Characterization*, vol. 101, pp. 34–39, 2015.
- [36] M. Nath and H. S. Tripathi, "Thermo-mechanical behavior of Al<sub>2</sub>O<sub>3</sub>-Cr<sub>2</sub>O<sub>3</sub> refractories: effect of TiO<sub>2</sub>," *Ceramics International*, vol. 41, no. 2, pp. 3109–3115, 2015.
- [37] J. Zhang, *Preparation, Growth Methenism of Mullite Whiskers and Their Enhancement Effect on Ceramic Matrix composites*, China University of Geosciences, Wuhan, 2012.
- [38] X. Ma, T. Ohtsuka, S. Hayashi, and Z.-e. Nakagawa, "The effect of BN addition on thermal shock behavior of fiber reinforced porous ceramic composite," *Composites Science and Technology*, vol. 66, no. 15, pp. 3089–3093, 2006.
- [39] K. K. Chawla, "Interface engineering in mullite fiber/mullite matrix composites," *Journal of the European Ceramic Society*, vol. 28, no. 2, pp. 447–453, 2008.
- [40] T. Zhang, L. Kong, Z. Du, J. Ma, and S. Li, "Tailoring the microstructure of mechanoactivated Al<sub>2</sub>O<sub>3</sub> and SiO<sub>2</sub> mixtures with TiO<sub>2</sub> addition," *Journal of Alloys and Compounds*, vol. 506, no. 2, pp. 777–783, 2010.
- [41] C. Liu, J. Chen, and W. Cai, "Data-Driven remanufacturability evaluation method of waste parts," *IEEE Transactions on Industrial Informatics*, vol. 18, no. 7, pp. 4587–4595, 2022.